Titanium Selenide Saturable Absorber Mirror for Passive Q-Switched Er-Doped Fiber Laser

Wenjun Liu, Mengli Liu, Ming Lei, Shaobo Fang, and Zhiyi Wei

(Invited Paper)

***Abstract*—Titanium selenide saturable absorber mirror ($TiSe_2$-SAM) is fabricated by a combination of magnetron sputtering method and chemical vapor deposition method. With the optical circulator, the $TiSe_2$-SAM is flexibly injected in the experimental cavity as the saturated absorber, and a steady Q-switched Er-doped fiber (EDF) laser is established. The modulation depth of $TiSe_2$-SAM is measured to be 25.92%. Through appropriately adjusting the polarization states and changing the pump power, the shortest pulse duration and maximum output power of the passive Q-switched EDF laser are 1.126 μs and 11.54 mW, respectively. The adjustable range of the repetition rate is 70–154 kHz, and the signal to noise ratio is greater than 62 dB. To our best knowledge, there is no report on Q-switched EDF lasers based on $TiSe_2$ up to now, and our new attempt on $TiSe_2$-based Q-switched EDF laser proves that $TiSe_2$ as a powerful candidate is promising in ultrafast optical generation for the characteristics of high modulation depth and high stability.**

***Index Terms*—Nonlinear optical materials, fiber laser, Q-switched lasers.**

I. Introduction

Transition metal dichalcogenides (TMDs), as graphene-like two-dimensional materials, have received extensive attention on account of their unique electrical and optical saturable absorption properties [1]. However, compared with graphene, which has a gapless Dirac cone band structure, the relatively large modulation depth of TMDs makes it more flexible to be applied in optoelectronic and photonic devices. Layered TMDs have similar chemical expressions as MX_2 (M common are Mo, W, and X are generally S, Se, Te), which are connected by weak van der Waals forces [3]–[5]. Optical measurements have experimentally supported that the transition from indirect to direct bandgap occur simultaneously when monolayer limit is broken [6]–[10]. Furthermore, the charge carriers are feasible to be optically controlled in two energy degraded conductive valleys and valence bands at corners of the first Brillouin zone. In other words, high-quality layered TMDs have excellent properties such as ultrafast electron relaxation time and large modulation depth [11]–[13].

As far as we know, most materials of the TMDs family have been fully investigated in optics operations as SAs. The demonstrations of WS_2 and MoS_2 based mode-locked and Q-switched lasers with characteristics of ultrafast photonic and broadband have been reported [14]–[23]. Compared with WS_2 and MoS_2, $MoSe_2$ with narrower bandgap makes it more applicable in broadband saturable absorption for ultrafast pulsed laser [24]–[26]. On the other hand, as a member of the TMDs family, $TiSe_2$ has not been applied in optical equipment. Compared with other members of TMDs, the band gap of $TiSe_2$ is 0.15 eV, so it is more advantageous in terms of broadband absorption [27]–[28].

Magnetron sputtering method, pulsed laser deposition (PLD) and chemical vapor deposition (CVD) process are several frequently-used methods to employ in the manufacture of SAs, but the attempt to combine two or more approaches in the fabrication of SAs is scarcely reported yet. The $TiSe_2$-SAM is prepared by a combination of magnetron sputtering method and CVD method. The magnetron sputtering method with advantages of simple equipment, large coating scale and strong adhesion, is used to spray a 200 nm-thick gold film on a SiO_2/Si substrate to form a mirror. The CVD process is chosen to grow $TiSe_2$ film on the surface of gold mirror. CVD process as a relatively mature production method is able to precisely control the orientation, growth, structure, and morphology of films [29]–[32]. Through combining two methods, the gold film with large scale and $TiSe_2$ film with high purity are both obtained. This hybrid coating method not only brings SAs with high purity, but also greatly reduces the cost of production. The double-balanced detection method is used to measure the saturable absorption properties of the material, the modulation depth of the $TiSe_2$-SAM is measured to be 25.92%. Corresponding, the saturable loss and absorption intensity can also be measured to be 44.97% and 13.211 MW/cm^2.

Highly stable Q-switched fiber laser with the high signal to noise ratio (SNR) of 62 dB, maximum output power of

Manuscript received July 14, 2017; revised September 17, 2017; accepted September 30, 2017. Date of publication October 5, 2017; date of current version October 27, 2017. This work was supported in part by the National Key Basic Research Program of China under Grants 2012CB821304, 2013CB922401, and 2013CB922402, in part by the National Natural Science Foundation of China under Grants 11674036, 61378040, 61575219, and 11078022, and in part by the Fund of State Key Laboratory of Information Photonics and Optical Communications, Beijing University of Posts and Telecommunications under Grant IPOC2016ZT04. *(Corresponding authors: Ming Lei and Zhiyi Wei.)*

W. Liu, M. Liu, and M. Lei are with the State Key Laboratory of Information Photonics and Optical Communications, School of Science, Beijing University of Posts and Telecommunications, Beijing 100876, China (e-mail: jungliu@bupt.edu.cn; mengliliu@bupt.edu.cn; mlei@bupt.edu.cn).

S. Fang and Z. Wei are with the Beijing National Laboratory for Condensed Matter Physics, Institute of Physics, Chinese Academy of Sciences, Beijing 100190, China (e-mail: shaobo.fang@iphy.ac.cn; zywei@iphy.ac.cn).

Color versions of one or more of the figures in this paper are available online at http://ieeexplore.ieee.org.

Digital Object Identifier 10.1109/JSTQE.2017.2759266

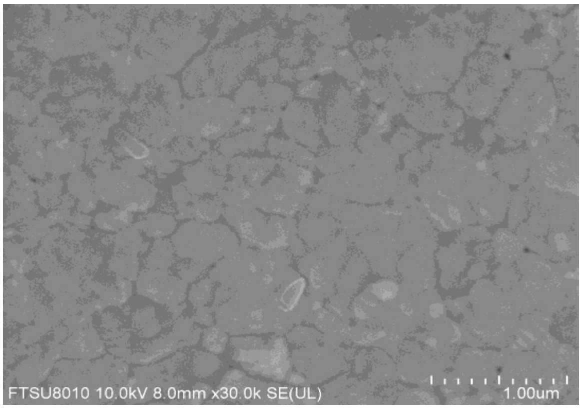

Fig. 1. SEM image of the $TiSe_2$-SAM with solution of 1 μm.

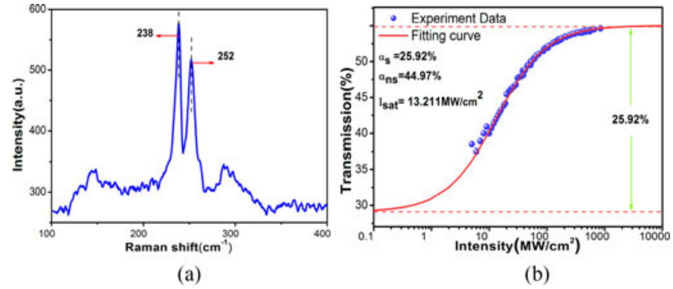

Fig. 2. (a) Raman spectra analysis. (b) Nonlinear saturable absorption of the $TiSe_2$-SAM. The modulation depth is 25.92%, the saturation intensity is 13.211 MW/cm^2, and the non-saturable loss is 44.97%.

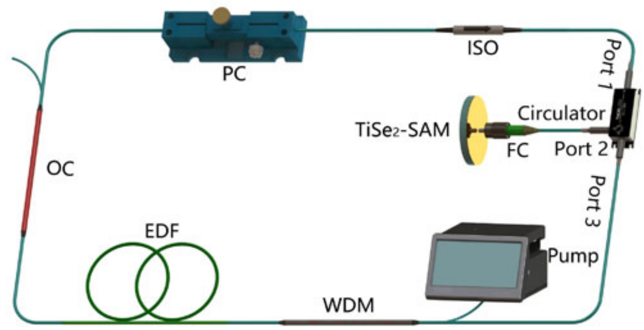

Fig. 3. Schematic diagram of experiment based on the $TiSe_2$-SAM. The included components are: wavelength division multiplexer (WDM), optic circulator (Circulator), the erbium-doped fiber (EDF), pump, optical coupler (OC), polarization controller (PC), titanium selenide saturable absorber mirror ($TiSe_2$-SAM), isolator (ISO).

11.54 mW and shortest pulse duration of 1.126 μs is achieved in this paper. When the pump power changes within 630 mW to 192 mW, the Q-switched repetition rate is adjustable over a range which is from 154 kHz to 70 kHz. This is the first attempt of $TiSe_2$ in the Q-switched operations as a SA. These experimental data indicate that $TiSe_2$ SA made by conjoint method is a promising material to achieve highly stable Q-switched fiber laser.

II. Experimental Results

A. Fabrication and Characterization of $TiSe_2$-SAM

The gold film is deposited on SiO_2/Si substrate by magnetron sputtering technique to form gold mirror. Then CVD process is employed to grow ultrathin $TiSe_2$ film on gold mirror. Prior to deposition, the vacuum chamber is evacuated to a vacuum of $\sim 1 \times 10^{-4}$ Pa. The argon flow is 20 sccm and the current is 0.4 A. 3 minutes later, the $TiSe_2$-SAM with two functions of saturable absorption and reflection is ready. The CVD method is applied in this manufacture for several advantages. The direction of crystal growth, structure and morphology of materials are effectively controlled in CVD. Moreover, the crystal film grown in this way brings a higher level of purity.

For a more detailed observation of microstructure of the $TiSe_2$-SAM, scanning electron microscopy (SEM) image with the high resolution of 1 μm is caught. As it presented in Fig. 1, uniform particles of $TiSe_2$ are tightly attached to the surface of the gold mirror. In order to figure out the phonon spectra properties of the $TiSe_2$-SAM, further utilization of Raman spectra is needed. Two main peaks in the range of 200–300 cm^{-1} are observed in Fig. 2(a). The previous $TiSe_2$ flakes reveal two Raman peaks at $\sim$134 cm^{-1} and $\sim$198 cm^{-1}, which are corresponded to E_g and A_{1g} modes. A certain degree of deviation is subsistent in our Raman spectra in comparison with the previous researches.

The measurement of absorption characteristics of the $TiSe_2$-SAM we adopted is the double-balanced detection method. The pumping source is a home-made fiber laser with the central wavelength of 1550 nm, pulse duration of 600 fs and repetition rate of 131 MHz. Part of which is measured directly by power meter and the other is measured after SA's saturable absorption. The function curve presented in Fig. 2(b) is consistent with the formula

$$\alpha(I) = \alpha_s / (I + I_{\rm sat}) + \alpha_{\rm ns},$$

Where α_s, $\alpha_{\rm ns}$ and $I_{\rm sat}$ are saturable absorption, nonsaturable absorption and saturation intensity, respectively. Under the influence of the weak light, the absorption effect of the $TiSe_2$-SAM is striking. Under the action of the intense light, the absorption tends to be saturated. This illustrates a typical saturable absorption property of the $TiSe_2$-SAM. The modulation depth of the $TiSe_2$-SAM is measured to be 25.92%. Corresponding, the saturable loss and absorption intensity can also be measured, they are 44.97% and 13.211 MW/cm^2, respectively.

B. Experimental Process of Q-Switched EDF Laser Based on $TiSe_2$-SAM

The experimental device diagram of the passively Q-switched EDF laser is shown in Fig. 3, a typical ring cavity based on the $TiSe_2$-SAM is used to realize the Q-switching operation. A 40 cm long Er-doped fiber (EDF) (Liekki 110 -4/125) is pumped persistently by the laser diode which is operating at the central wavelength of 976 nm. The optical coupler (OC) divides optical path into 80:20, 20% of which is extracted for the measurement of experimental results. The single mode fibers exhibit birefringence due to unexpected changes in the shape of the fiber core and anisotropic stresses. This undesired state causes two

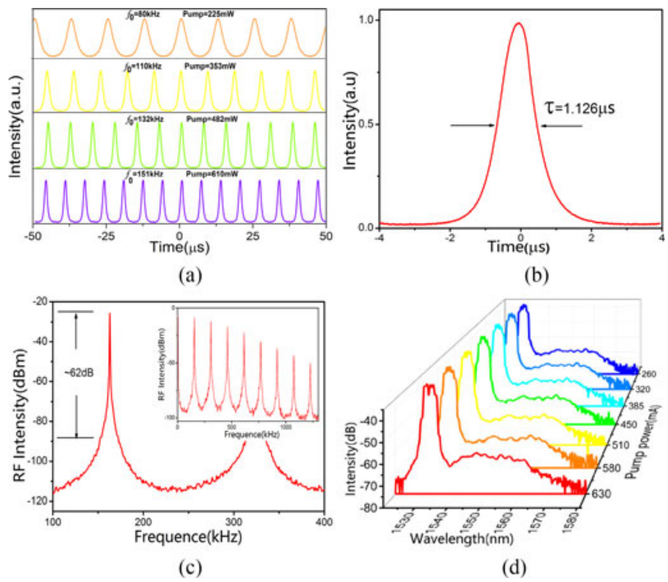

Fig. 4. Experimental results of the passively Q-switching fiber laser with the $TiSe_2$-SAM. (a) Q-switched pulse train at different pump powers. (b) Single pulse image of the Q-switched fiber laser. (c) Radio frequency spectrum measured with 3 Hz RBW. (d) Spectrum of the Q-switching pulse train at different pump powers.

orthogonal polarization modes to influence each other because of additional phase differences during transmission. PC is able to control the polarization state of the light, which partly counteract the influence of birefringence and optimize the performance of the laser. The unrequired light echo from ring cavity can be avoided by isolator (ISO). The $TiSe_2$-SAM comprises a three-tier structure, which is made up of the substrate, gold film and $TiSe_2$ film. The role of the gold film is to reflect the light after the interaction with $TiSe_2$. The optical circulator is a three-port device, and the light travels only in one direction. Light from the ISO is injected from port 1 of optical circulator, and ejected from port 2. After that, light interacts with $TiSe_2$ fully, and then is reflected back to port 2 by the gold film. At last, light enters the ring cavity from port 3. The optical spectrum is monitored by an optical spectrum analyzer (Yokogawa AQ6370C) and the output pulse train is indicated by a 250 MHz oscilloscope (Tektronix DPO3054). The analysis of frequency domain and autocorrelation parameter can also be informed by the radio frequency spectrum analyzer and optical intensity autocorrelator.

As the pump power continues to increase, we observed Q-switched phenomenon when pump power is 192 mW. As long as the pump power is above this threshold, a stable output pulse train can be maintained. As presented in Fig. 4(a), when pump power is set to be 225 mW, 353 mW, 482 mW and 610 mW, the corresponding repetition rate are 80 kHz, 110 kHz,132 kHz and 151 kHz, respectively. Due to the limit of pump, the maximum pump power we employ is 630 mW, the output properties are summarized in Fig. 4(b)–(d). The symmetrical Gaussian waveform shows the shortest pulse duration of 1.126 μs as presented in Fig. 4(b), the corresponding repetition rate and output power are 154 kHz and 11.54 mW, respectively. To prove the high stability of the passively Q-switched fiber laser, the radio frequency (RF) output spectra is measured as shown in Fig. 4(c). With the resolution bandwidth (RBW) of 3 Hz and span of 300 kHz, the SNR is superior to 62 dB, and the waveform is relatively smooth, there is no obvious interference frequency component produced. For the insert figure of Fig. 4(c) in a wide range, the adopted parameters of the RBW and span are 300 Hz and 1.3 MHz, respectively. The illustration shows a rigorous wide range declining trend of harmonic frequency, which indicates the Q-switched laser is in a stable working state. The Q-switched spectra under different pump powers are shown in Fig. 4(d), the operating wavelength of the stable Q-switched EDF laser is 1530 nm. As we can see from the diagram, the spectra under different powers have no obvious change, and the spectral width is kept at about 1.6 nm, which shows the stability of our Q-switched laser.

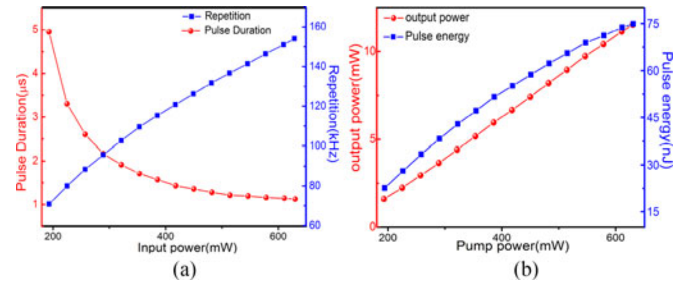

Fig. 5. (a) The duration and repetition rate with different pump powers. (b) The pulse energy and output power under different values of pump powers.

Since the output characteristics of the pulse can be affected by non-linear dynamics of SA, the pulse duration as well as repetition rate are related to the trend of the pump power as presented in Fig. 5(a). With the boosting of the pump power from 192 mW to 630 mW, there is a nearly monotonous increase of the repetition rate from 70 kHz to 154 kHz. In the initial stage of pump power growth, the sharp trend of the pulse duration is obvious, when the pump power continues to increase, the pulse duration tends to be stable, and the variation range is smaller, which indicates that the SA tends to be saturated. Moreover, during the change of the pump power, no interfering pulse intensity fluctuations are observed, which proves the high stability of passively Q-switched pulse output. In Fig. 5(b), the measured output power and pulse repetition rate as a function of the pump power are represented by curves, the variations of the pulse energy and output power are almost linear, which are typical performance of the passive Q-switched fiber laser.

III. Discussion

The band gap of $TiSe_2$ is smaller than that of some other TMDs, therefore it is able to achieve broadband absorption as graphene does. Table I shows the related optical parameters among different SAs. Obviously, the modulation depth of the $TiSe_2$-SAM is much higher than that of previous SAs. This indicates that $TiSe_2$ can partly compensate for the small modulation depth of other materials. We suspect it may be related to the way the material produced. The higher modulation depth may due mainly to the combination of two production methods,

TABLE I
COMPARISON OF PARAMETERS BETWEEN DIFFERENT SAS

SA type	Modulation depth	Saturable absorption intensity(MW/cm^2)	Un-saturated loss	Ref
Graphene	1.3%	–	–	34
SWNTs	0.94%	–	–	35
Bi_2Se_3	4.3%	11	–	36
Bi_2Te_3	22%	57	21%	37
WS_2	4.9%	3.83	3.65%	38
MoS_2	2%	10	–	39
WSe_2	3.5%	103.9	75.1%	40
$MoSe_2$	6.73%	132.5	39.2%	26
$TiSe_2$	25.92%	13.2	44.97%	This work

TABLE II
PERFORMANCE COMPARISON BETWEEN Q-SWITCHED EDF LASERS BASED ON DIFFERENT TWO-DIMENSIONAL MATERIALS

Materials	$\tau(\mu s)$	$f_{\rm rep}$ (kHz)	SNR(dB)	Ref
Graphene	3.89	10.36–41.8	30	33
Bi_2Se_3	1.9	459–940	50	36
Bi_2Te_3	14	2.15–12.8	36.4	37
WS_2	1.3	79–97	40	38
MoS_2	3.3	10.6–34.5	50	39
WSe_2	3.98	4.5–49.6	46.7	40
$MoSe_2$	4.04	60.7–66.8	31.3	26
$TiSe_2$	1.13	70–154	62	This work

magnetron sputtering method and CVD. This combination brings the advantage of higher purity of $TiSe_2$ film, this may explain the reason for the high modulation depth of $TiSe_2$-SAM. Moreover, the relatively low saturation intensity indicates the threshold of the laser is relatively small [36].

Table II demonstrates the performance comparison between Q-switched EDF lasers based on different 2D materials. It can be observed that the SNR of the $TiSe_2$-based Q-switched EDF laser is much higher than that of previous fiber lasers. This illustrates that our new application of $TiSe_2$ is beneficial to form a stable fiber laser. Therefore, $TiSe_2$ as a powerful candidate is promising in the ultra-fast optical field for the characteristics of high modulation depth and high stability.

IV. CONCLUSION

In conclusion, through the combination of magnetron sputtering method and CVD method, the gold film with large scale and $TiSe_2$ film with high purity have been both obtained. With the circulator, the $TiSe_2$-SAM has been flexibly injected in the experimental cavity as the SA, and the stable Q-switched EDF laser with the pulse duration range from 4.953 μs to 1.126 μs and repetition rates range from 70 kHz to 154 kHz has been established. The relatively high SNR of 62 dB has revealed high stability of the Q-switched EDF laser. Large modulation depth and stable short pulse generation indicate that $TiSe_2$ is a potential candidate for ultrafast fiber lasers. In our future work, material production process will be further optimized, more practical and excellent materials will be produced for ultrafast lasers.

REFERENCES

[1] B. Sivacarendran *et al.*, "Two-dimensional molybdenum trioxide and dichalcogenides," *Adv. Funct. Mater.*, vol. 23, no. 32, pp. 3952–3970, Jan. 2013.

[2] Y. Zhang *et al.*, "Direct observation of the transition from indirect to direct bandgap in atomically thin epitaxial $MoSe_2$," *Nat. Nanotechnol.*, vol. 9, no. 2, pp. 111–115, Dec. 2015.

[3] B. Radisavljevic, A. Radenovic, J. Brivio, V. Giacometti, and A. Kis, "Single-layer MoS_2 transistors," *Nat. Nanotechnol.*, vol. 6, no. 3, pp. 147–150, Jan 2011.

[4] M. Chhowalla *et al.*, "The chemistry of two-dimensional layered transition metal dichalcogenide nanosheets," *Nat. Chem.*, vol. 5, no. 4, pp. 263–275, Mar. 2013.

[5] K. Wu *et al.*, "High-performance mode-locked and Q-switched fiber lasers based on novel 2D materials of topological insulators, transition metal dichalcogenides and black phosphorus: Review and perspective," *Opt. Commun.*, 2017. [Online]. Available: https://doi.org/10.1016/j.optcom.2017.02.024

[6] K. F. Mak, C. Lee, J. Hone, J. Shan, and T. F. Heinz, "Atomically thin MoS_2: A new direct-gap semiconductor," *Phys. Rev. Lett.*, vol. 105, no. 13, Sep. 2010, Art. no. 136805.

[7] S. Tongay *et al.*, "Thermally driven crossover from indirect toward direct bandgap in 2d semiconductors: $MoSe_2$ versus Mos_2," *Nano Lett.*, vol. 12, no. 11, pp. 5576–5580, Oct. 2012.

[8] A. Splendiani *et al.*, "Emerging photoluminescence in monolayer MoS_2," *Nano Lett.*, vol. 10, no. 4, pp. 1271–1275, Mar. 2010.

[9] J. K. Ellis, M. J. Lucero, and G. E. Scuseria, "The indirect to direct band gap transition in multilayered MoS_2 as predicted by screened hybrid density functional theory," *Appl. Phys. Lett.*, vol. 99, no. 26, Dec. 2011, Art. no. 261908.

[10] A. Kumar and P. K. Ahluwalia, "Electronic structure of transition metal dichalcogenides monolayers 1H-MX_2 (M = Mo, W; X = S, Se, Te) from ab-initio theory: new direct band gap semiconductors," *Eur. Phys. J. B*, vol. 85, no. 6, pp. 1–7, Jun. 2012.

[11] J. S. Rhyee *et al.*, "High-mobility transistors based on large-area and highly crystalline CVD-grown $MoSe_2$ films on insulating substrates," *Adv. Mater.*, vol. 28, no. 12, pp. 2316–2321, Jan. 2016.

[12] C. T. Le *et al.*, "Impact of selenium doping on resonant second-harmonic generation in monolayer MoS_2," *ACS Photon.*, vol. 4, no. 1, pp. 38–44, Dec. 2016.

[13] R. Wang *et al.*, "Third-harmonic generation in ultrathin films of MoS_2," *ACS Appl. Mater. Interfaces*, vol. 6, no. 1, pp. 314–318, Dec. 2014.

[14] R. Khazaeinezhad *et al.*, "Passive Q-switching of an all-fiber laser using WS_2 deposited optical fiber taper," *IEEE Photon. J.*, vol. 7, no. 5, Sep. 2015, Art. no. 1503507.

[15] K. Wu, X. Zhang, J. Wang, X. Li, and J. Chen, "WS_2 as a saturable absorber for ultrafast photonic applications of mode-locked and Q-switched lasers," *Opt. Express*, vol. 23, no. 9, pp. 11453–11461, Apr. 2015.

[16] M. Zhang *et al.*, "Yb- and Er-doped fiber laser Q-switched with an optically uniform, broadband WS_2 saturable absorber," *Sci. Rep.*, vol. 5, Dec. 2015, Art. no. 17482.

[17] H. Ahmad *et al.*, "Passively Q-switched erbium-doped fiber laser at C-band region based on WS_2 saturable absorber," *Appl. Opt.*, vol. 55, no. 5, pp. 1001–1005, Feb. 2016.

[18] W. Liu *et al.*, "Tungsten disulfide saturable absorbers for 67 fs mode-locked erbium-doped fiber lasers," *Opt. Express*, vol. 25, no. 3, pp. 2950–2959, Feb. 2017.

[19] W. Liu *et al.*, "Tungsten disulphide for ultrashort pulse generation in all-fiber lasers," *Nanoscale*, vol. 9, no. 18, pp. 5806–5811, May 2016.

[20] Z. Tian *et al.*, "Mode-locked thulium fiber laser with MoS_2," *Laser Phys. Lett.*, vol. 12, no. 6, Jun. 2015, Art. no. 065104.

[21] H. Xia *et al.*, "Ultrafast erbium-doped fiber laser mode-locked by a CVD-grown molybdenum disulfide (MoS_2) saturable absorber," *Opt. Express*, vol. 22, no. 14, pp. 17341–17348, Jul. 2014.

[22] J. Du *et al.*, "Ytterbium-doped fiber laser passively mode locked by few-layer molybdenum disulfide (MoS_2) saturable absorber functioned with evanescent field interaction," *Sci. Rep.*, vol. 4, Sep. 2014, Art. no. 6346.

[23] Z. Luo *et al.*, "1-, 1.5-, and 2-μm fiber lasers Q-switched by a broadband few-layer MoS_2 saturable absorber," *J. Lightw. Technol.*, vol. 32, no. 24, pp. 4077–4084, Dec. 2014.

[24] S. Tongay *et al.*, "Thermally driven crossover from indirect toward direct bandgap in 2D semiconductors: $MoSe_2$ versus MoS_2," *Nano Lett.*, vol. 12, no. 11, pp. 5576–5580, Oct. 2012.

[25] Z. Luo *et al.*, "Two-dimensional material-based saturable absorbers: Towards compact visible-wavelength all-fiber pulsed lasers," *Nanoscale*, vol. 8, no. 2, pp. 1066–1072, Nov. 2015.

[26] B. Chen *et al.*, "Q-switched fiber laser based on transition metal dichalcogenides MoS_2, $MoSe_2$, WS_2, and WSe_2," *Opt. Express*, vol. 23, no. 20, pp. 26723–26737, Oct. 2015.

[27] J. C. E. Rasch, T. Stemmler, B. Müller, L. Dudy, and R. Manzke, "1T–$TiSe_2$: Semimetal or semiconductor," *Phys. Rev. Lett.*, vol. 101, no. 23, Dec. 2008, Art. no. 237602.

[28] P. Chen *et al.*, "Charge density wave transition in single-layer titanium diselenide," *Nat. Commun.*, vol. 6, Nov. 2015, Art. no. 8943.

[29] W. Zhang *et al.*, "High-gain phototransistors based on a CVD MoS_2 monolayer," *Adv. Mater.*, vol. 25, no. 25, pp. 3456–3461, May 2013.

[30] N. P. Lopez *et al.*, "Photosensor device based on few-layered WS_2 films," *Adv. Funct. Mater*, vol. 23, no. 44, pp. 5511–5517, Jun. 2013.

[31] J. K. Huang *et al.*, "Large-area synthesis of highly crystalline WSe_2 monolayers and device applications," *ACS Nano*, vol. 8, no. 1, pp. 923–930, Dec. 2013.

[32] Y. H. Chang *et al.*, "Monolayer $MoSe_2$ grown by chemical vapor deposition for fast photodetection," *ACS Nano*, vol. 8, no. 8, pp. 8582–8590, Aug. 2014.

[33] J. Wang *et al.*, "Evanescent-light deposition of graphene onto tapered fibers for passive Q-switch and mode-locker," *IEEE Photon. J.*, vol. 4, no. 5, pp. 1295–1305, Oct. 2012.

[34] S. Kivistö, T. Hakulinen, A. Kaskela, and B. Aitchison, "Carbon nanotube films for ultrafast broadband technology," *Opt. Express*, vol. 17, no. 4, pp. 2358–2363, Feb. 2009.

[35] Z. Sun *et al.*, "Graphene mode-locked ultrafast laser," *ACS Nano*, vol. 4, no. 2, pp. 803–810, Jan. 2010.

[36] Z. Yu *et al.*, "High-repetition-rate Q-switched fiber laser with high quality topological insulator Bi_2Se_3 film," *Opt. Express*, vol. 22, no. 10, pp. 11508–11515, Oct. 2014.

[37] Y. Chen *et al.*, "Large energy, wavelength widely tunable, topological insulator Q-switched erbium doped fiber laser," *IEEE J. Sel. Topics Quantum*, vol. 20, no. 5, pp. 315–322, Sep./Oct. 2014.

[38] M. Zhang *et al.*, "Yb- and Er-doped fber laser Q-switched with an optically uniform, broadband WS_2 saturable absorber," *Sci. Rep.*, vol. 5, Dec. 2015, Art. no. 17482.

[39] Y. Huang *et al.*, "Widely-tunable, passively Q-switched erbium-doped fiber laser with few-layer MoS_2 saturable absorber," *Opt. Express*, vol. 22, no. 21, pp. 25258–25266, Oct. 2014.

[40] B. Chen *et al.*, "Tungsten diselenide Q-switched erbium-doped fiber laser," *Opt. Eng.*, vol. 55, no. 8, Jan. 2016, Art. no. 081306.

Wenjun Liu received the Ph.D. degree from Beijing University of Posts and Telecommunications, Beijing, China, in 2011. He was a Postdoctoral fellow in the Laboratory of Optical Physics, Institute of Physics, Chinese Academy of Sciences from 2012 to 2015. He is currently an Associate Professor at Beijing University of Posts and Telecommunications. His research interests include ultrafast and ultrahigh intensity laser technology, and advanced material for ultrafast photonics.

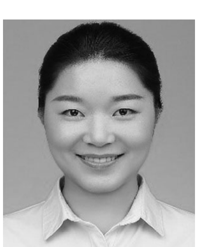

Mengli Liu received the Bachelor's degree in communications engineering from South-Central University for Nationalities, Wuhan, China, in 2016. She is currently working toward the Ph.D. degree at the Department of Electronic Science and Technology, Beijing University of Posts and Telecommunications, Beijing, China. Her research interests include ultrafast fiber laser and two-dimensional nanomaterials.

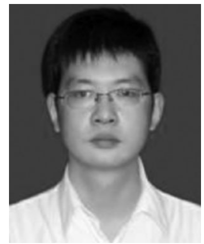

Ming Lei received the Ph.D. degree from Institute of physics, Chinese Academy of Science, Beijing, China, in 2007. He worked as a postdoctoral fellow at the Hong Kong University of Science and Technology and Chinese University of Hong Kong from 2007 to 2008 and from 2009 to 2010, respectively. He is currently a Professor with Beijing University of Posts and Telecommunications, Beijing, China. His research work focuses on optoelectronic materials and devices.

Shaobo Fang received the Ph.D. degree from Hokkaido University, Sapporo, Japan. From 2007 to 2011, he was an Assistant Research Scientist of the Core Research for Evolutional Science and Technology, Japan Science and Technology Agency. Since 2011, he has been a Research Scientist in the framework of the Helmholtz Association Young Scientist Program at DESY/CFEL, Hamburg, Germany. He joined the Key Laboratory of Optical Physics as Associate Professor in the Institute of Physics, Chinese Academy of Sciences, in 2015. He published more than 40 papers in leading technical journals and international conferences. His research interests include novel subcycle waveform synthesis for attosecond science, compact X-ray sources and advanced material for ultrafast photonics.

Zhiyi Wei received the Ph.D. degree, in 1991. After two years postdoctoral fellow at Sun Yat-Sen (Zhongshan) University in China, he worked at the Rutherford Appleton Lab in U.K., the Chinese University of Hong Kong, the Hong Kong University of Science and Technology, University of Groningen in the Netherland as a visiting scholar during 1993–1997. He joined in the Laboratory of Optical Physics, Institute of Physics, Chinese Academy of Sciences (CAS), in 1997. From April 2000 to Sept 2002, he also worked in the Advanced Industrial Science and Technology, in Japan as a NEDO Researcher. He was promted as an Assoicate Professor and a Full Professor in 1993 and 1999, respectively. His research interests focuses on ultrafast and ultrahigh intensity laser technology. Since 1985, he has made a series of innovation progresses on generation, synchronization, amplification; frequency conversion, and carrier envelop phase control of femtosecond laser. He also established the first domestic attosecond laser facility. Up to now, he has published more than 300 peer-reviewed papers, organized three international conferences as co-chairs (such 10th International Conference on Ultrafast Optics, 6th International Conference on Attosecond Physics). He received the State Natural Science Award (2nd-Class), the Excellent Achievements (team) and Contributions (2nd-Class) for Science and Technology by CAS. He also received the Young Scientist Prize by CAS in 2001, Young Distinguish Scholar Funding by NFSC in 2002, Hu Gangfu Prize by the Chinese Physical Society in 2011. He was elected as OSA fellow in 2016.